A comparison of porosity values inferred from magnetotelluric and bore-hole density data; case studies from two geothermal regions in South Australia

Thesis submitted in accordance with the requirements of the University of Adelaide for an Honours Degree in Geophysics.

Philippa Murray

October 2012

THE UNIVERSITY of ADELAIDE

ABSTRACT

Porosity is one of the main determining factors of the prospectivity of geothermal regions and can be estimated in a number of ways from geophysical surveys. The objective of this work was to better understand the link between porosity, permeability and electrical resistivity through Archie's law. This was achieved by comparing porosity values derived from magnetotelluric (MT) data with those derived from density measurements taken in a petroleum borehole. Two case studies were used and are located in north-eastern South Australia. The outcomes of these studies will help to minimise exploration risk by proving the effectiveness of MT as a primary survey of geothermal regions. This study provides a stepping stone to understand the ways in which permeability can be determined from MT surveys in order to better quantify expected fluid flow rates in geothermal prospects.

KEYWORDS

Porosity, Geothermal, Magnetotellurics, Resistivity, Density, Archie's law, permeability.

Table of Contents

List of Figures

List of Tables

INTRODUCTION

Geothermal is an increasingly important source of energy due to its sustainable nature and minimal environmental impacts. It is important to be able to refine exploration targets to reduce exploration costs and to help ensure the economic success of drilling programs. One of the largest problems faced by companies investing in geothermal projects in South Australia are lower than expected fluid flow rates. The relationship between the porosity and permeability of rock and electromagnetic resistivity is complex. Gaining a better understanding of the link will allow for more efficient exploration of geothermal regions and a knowledge of anticipated fluid flow rates. This project aims to better understand the link between porosity, permeability and electrical resistivity.

Magnetotellurics (MT) is a natural source electromagnetic method of imaging the electrical resistivity of the Earth's subsurface (Simpson & Bahr 2005). MT, like other geophysical techniques cannot determine lithology, instead it can provide information on physical properties such as salinity, porosity, permeability, melt fraction and viscosity (Bedrosian 2007). These properties are defined due to the changes they create in the resistivity profile through the subsurface.

Archie's Law (Archie 1942) is an empirical relationship which relates the in-situ resistivity to set physical properties and variables of sedimentary rocks. The equation defining the law has a number of variables which are representative of different properties of the rock (Sheriff 2002; Glover 2010). Implicit in this equation is the relationship between porosity and permeability. Chilingar et al. (1963) undertook a laboratory based investigation on this relationship and determined that in sands and sandstones there is an approximately logarithmic relationship between the two; ($\log(\text{permeability}) \approx \text{porosity}$). As this data was taken in a lab it cannot accurately determine an in-situ relationship. Leary & Al-Kindy (2002) discovered the same approximate relationship between porosity

and permeability in sediments extracted from well logs of the Brae oil-field. Normalised data showed an 80% correlation between fluctuations in log(permeability) and porosity.

Berryman (2003) suggests that only porosity can be measured from methods which measure electrical resistivity as both porosity and resistivity are scale invariant properties while permeability is not invariant. Permeability depends on both porosity and pore connectivity and also the scale of grain or pore sizes. Berryman (2003) states that because of these dependencies, porosity and thus electrical resistivity is not sufficient to determine the permeability of a rock. A second measurement is required which determines an appropriate length scale. Spichak & Manzella (2009) state that if the interconnected pore spaces are not damaged in the course of rock deformation the permeability can be determined from Archie's law.

In this study I aim to investigate the relationship between the porosity and permeability of two geothermally prospective regions in South Australia using MT (Figure 1). This will be done by comparing the results of MT surveys of the case studies with petroleum borehole data for the area. The comparison between borehole and MT data should provide enough variables to accurately constrain the porosity and provide an estimate of the permeability of the rock units.

BACKGROUND INFORMATION

Geothermal energy is fast becoming one of the most important types of clean, sustainable energy. There are three important components to consider when searching for prospective geothermal regions. These are; a source of heat, a reservoir and an insulating layer to keep the heat from escaping the Earth (Meju 2002). In order to ensure an economic discovery the region must also have the capacity for fluid flow, knowledge of which is gained through the permeability of the reservoir. Hot sedimentary aquifers, engineered geothermal systems and hydrothermal systems are the three predominant types

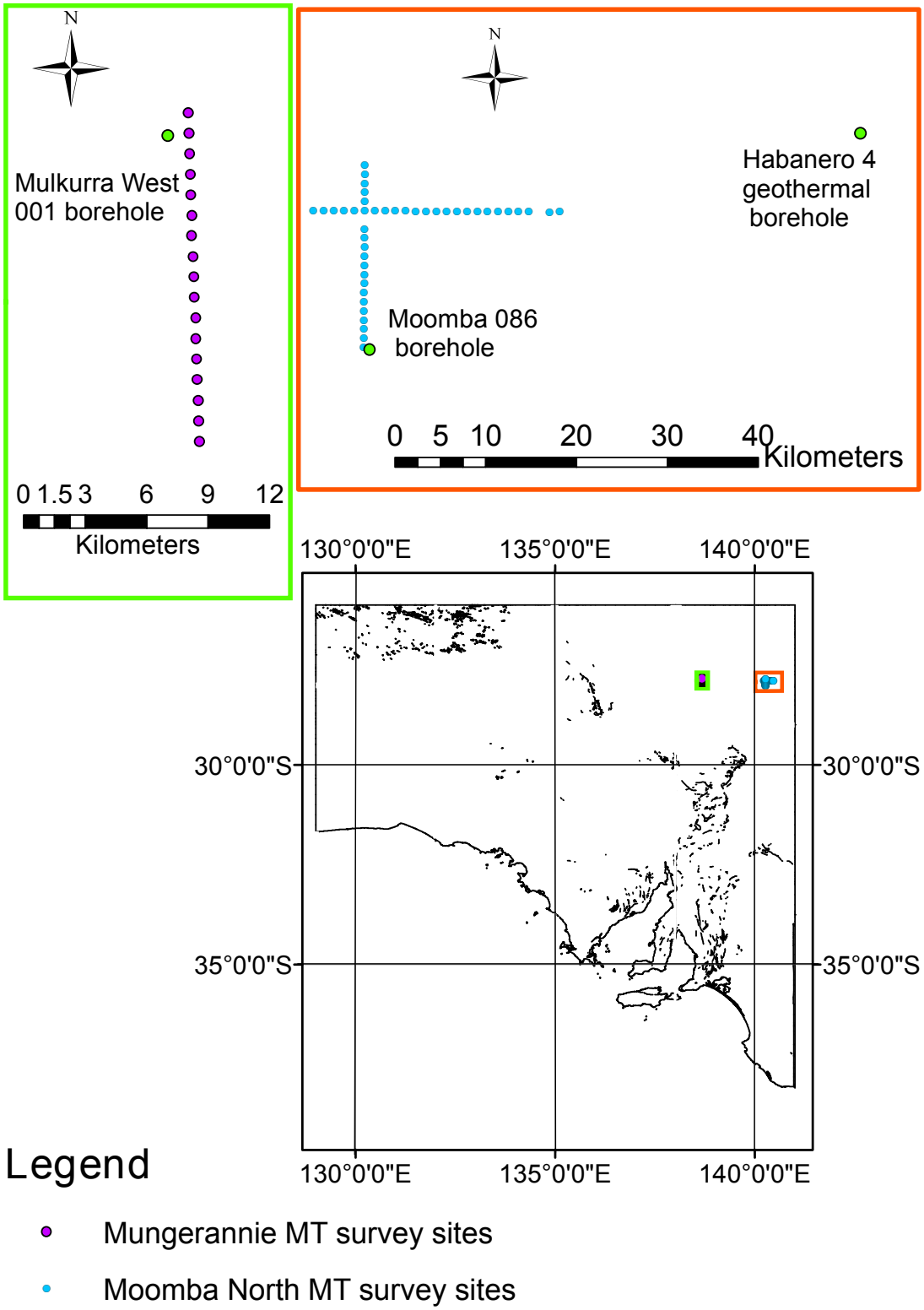

Figure 1: Locations and orientations of the two magnetotelluric surveys and petroleum and geothermal boreholes. The lower map shows the locations on the surveys within South Australia while the green upper box shows the orientation of the Mungerannie survey within the green box shown in the lower map; the location of the Mulkurra west 001 borehole is shown in relation to the MT survey. The upper orange box shows the orientation of the Moomba North MT survey with the relative locations of the Moomba 086 borehole and the Habanero 4 geothermal borehole.

of geothermal systems found worldwide (Ledru & Frottier 2010). Owing to the tectonic stability of Australia, hydrothermal systems, in which permeability is normally high, are very rare and are not considered further in this study. Hot sedimentary aquifers (HSA) consist of the three components mentioned previously in order to be prospective but are not necessarily permeable. Engineered geothermal systems (EGS) comprise only a source of heat and an insulating layer. Both of these systems generally require "fracking" to increase permeability and EGS systems further require fluid to be injected into the system. Knowledge of the porosity and permeability is crucial to aid in the determination of the system type and has implications for the scale and cost of an operation. At present one of the largest problems faced by companies investing in geothermal projects are low fluid flow rates in EGS systems. Porosity is known to be readily identifiable from magnetotelluric surveys however the recognition and quantification of permeability is an area of research pivotal to the effective identification of prospective geothermal reservoirs (Berryman 2003; Chilingar et al. 1963).

Permeability is defined as the measure of the ease with which a fluid can pass through the pore spaces of a formation (Sheriff 2002). The SI unit is m^2, however it is often denoted in units of millidarcy (1 $darcy \approx 10^{-}12m^2$). Permeability is defined as:

$$\kappa = \frac{\mu q}{dp/dx} \tag{1}$$

where:

κ is permeability

μ is fluid visciosity (units: Nsm^{-2})

q is linear rate of flow (units: ms^{-1})

dp/dx is the hydraulic pressure gradient (units: Nm^{-3})

The relationship between permeability and flow rate is what makes permeability such an important factor in the search for prospective geothermal regions. Accurate quantification of permeability can determine if sustainable fluid flow will be at a level which is high enough to be economic. Geodynamics (in a joint venture with Origin Energy) drilled proof of concept wells in the Cooper Basin (Figure 1) and have established through flow tests that in a 4 m thick rock package there are 28 mm of open fractures (Wyborn, pers. comm.).

The two magnetotelluric case studies presented in this paper are within the South Australian Heat Flow Anomaly (SAHFA) (Neumann et al. 2000) and and were undertaken by Quantec Geoscience for Eden Energy as the stratigraphy was considered to indicate prospectivity. The exploration leases have since expired and were not renewed due to the lack of prospectivity and feasibility of a venture. The surveys are located near the western edge of the Cooper Basin. The first study comprises the Moomba North MT survey, a survey constructed of two perpendicular lines oriented N-S and E-W. The N-S line will be used in this investigation. It is compared to data from the Moomba 086 petroleum borehole, with logged depths from around 2100 m to 2900 m. The second study uses the Mungerannie MT survey which is constructed of one N-S oriented line. This will be compared to data from the Mulkurra West 001 petroleum borehole, covering logged depths from roughly 850 to 1300 m.

MT is a natural source electromagnetic method of imaging the Earth's surface. It relies on natural magnetic fields which induce electric fields to determine the resistivity or conductivity of the earth. Orthogonal measurements of electric and magnetic field variations at the surface determine the resistivity (Simpson & Bahr 2005). In a two-dimensional earth the transverse electric (TE) mode describes the electric field parallel to the strike (some form of vertical resistivity boundary) and the transverse magnetic (TM) mode describes currents flowing perpendicular to strike. As the case studies are

both in regions considered to be one-dimensional there is no strike direction and the two modes can be oriented in any horizontal mutually perpendicular directions. The impedance tensor (Z) relates the orthogonal components of the horizontal electric (**E**) and magnetic (**H**) fields.

$$\mathbf{E} = \begin{pmatrix} Z_{xx} & Z_{xy} \\ Z_{yz} & Z_{yy} \end{pmatrix} \mathbf{H} \tag{2}$$

In a 1-D earth the diagonal elements equal zero; $Z_{xx} = Z_{yy} = 0$, while the off diagonal elements are non-zero and equal; $Z_{xy} = Z_{yx} \neq 0$. The impedance tensor is complex and thus has magnitude and phase. The magnitude of the tensor is the apparent resistivity; ρ_a, which describes the average resistivity of an equivalent half space. The phase; ϕ, gives the phase difference between the electric and magnetic fields.

The bulk electrical resistivity of earth materials varies over 10 orders of magnitude. For land based MT surveys a range of three to four orders of magnitude variation in resistivity is expected, compared to seismic velocities which vary only by a factor of 10 or rock densities which vary by a factor of three (Bedrosian 2007). The large variation in measurement range means MT can have a more discerning view of the subsurface in which small changes are detectable.

Interpretation of MT profiles must be undertaken with care as highly compacted clays give an almost identical resistivity profile as highly porous sandstone due to the high conductivity of connected clay minerals. Exploration for conventional geothermal systems typically makes use of clay in the system as it is often the cap of a reservoir and makes an easily identifiable target (Heise et al. 2008). In the interpretation of EGS systems a clay cap is a hindrance as it distorts the view of underlying sediments.

Archie's law (Archie 1942) is an empirical relationship, comprised of two sections which relate the in-situ resistivity of sedimentary rocks to their porosity and water saturation

$$F = \frac{R_O}{R_W} = \frac{\phi^m}{a}, \tag{3}$$

$$\frac{R_O}{R_t} = S_W^n \tag{4}$$

where

F is the unit-less formation factor

R_O is the resistivity of the formation when 100% saturated with water (units: Ωm)

R_W is the resistivity of water (units: Ωm)

ϕ is the porosity (measured in %)

S_W is the water saturation of the pore space (measured in %)

R_t is the true resistivity of the formation (units: Ωm)

n is the saturation exponent (unit-less)

a is the tortuosity factor (unit-less) which corrects for variations in compaction, pore structure and grain size

m is the cementation factor (unit-less) which models how much the pore network increases the resistivity, this variable is related to permeability as increasing permeability leads to a lower cementation exponent.

The law does not work for rocks composed of clay minerals as it assumes the rock is composed of a non-conducting mineral matrix. The equations have a number of variables which represent different properties of the strata (Sheriff 2002; Glover 2010):

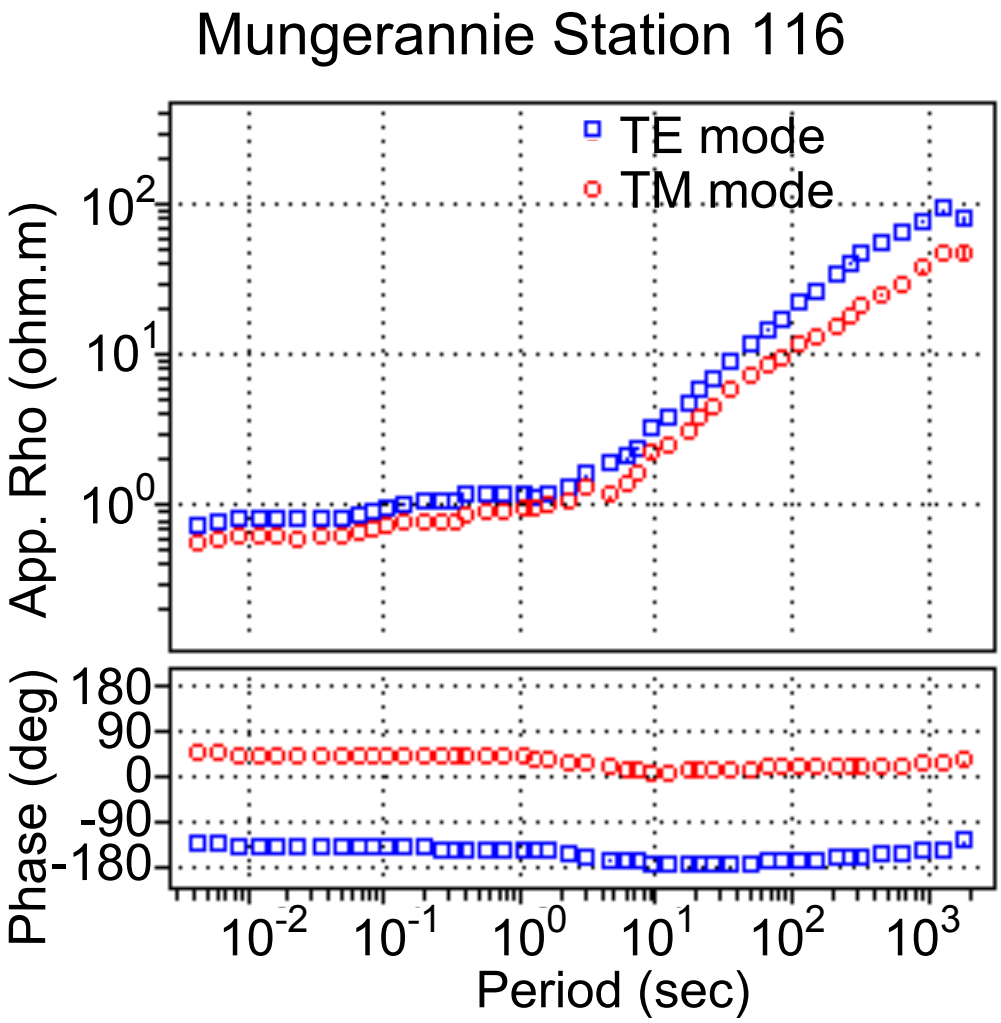

Figure 2: Typical apparent resistivity and phase for the Mungerannie MT survey. TE mode is shown by blue squares, TM mode by red circles. Resistivity values are taken from the *.edi files of the survey. For some stations of the survey certain outlier points of the plots were masked.

METHODS

Two Magnetotelluric surveys were interepreted using the information provided in the edi files for each station in each survey. The data had already been collected and processed by Quantec Geoscience (Stockill 2008) and the edi files are in the public domain and available on the South Australian Government's DMITRE SARIG website

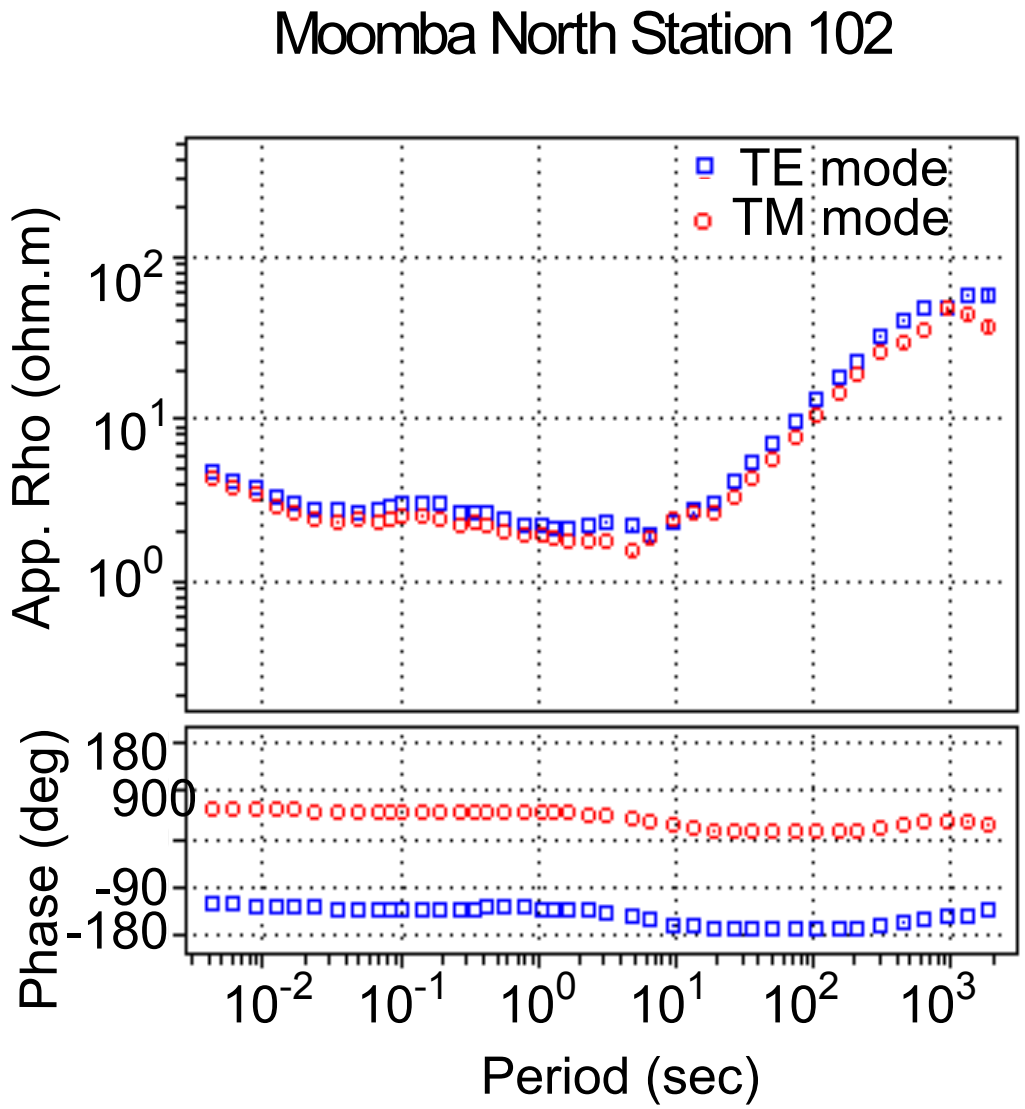

Figure 3: Typical apparent resistivity and phase for the Moomba North MT survey. TE mode is shown by blue squares, TM mode by red circles. Resistivity values are taken from the *.edi files of the survey. For some stations of the survey certain outlier points of the plots were masked.

(DMITRE 2012). As the data is from sedimentary basins it is assumed to be one-dimensional. One-dimensionality makes modelling of the data a relatively simple process; there is no need to rotate the data to the correct strike orientation to model it in a 2-D section as it is the same in all horizontal directions. The assumption is made valid by the apparent resistivity and phase diagrams (Figures 2 and 3). They show both TE and TM modes lying on top of one another for most of the apparent resisitivity curves.

The files were imported into WinGlink; a 2- and 3-D inversion modelling program. WinGlink was used to produce a 2-D MT inversion using a non-linear conjugate gradient algorithm (Mackie 2001). The models were produced by starting with a section of uniform conductivity of 10 Ωm and then setting pertinent parameters. Of particular importance to the final model were the allowable data error percentages and the smoothness factor τ. These parameters were reduced as the model was run through successive batches of iterations.

For the first inversion of each model the apparent resisitivity errors were set at 20% and the phase errors at 10% . The colour scale of the output was set as red-white-blue (red is conductive) with a logarithmic scale ranging in value from 1 to 10000 Ωm. The background resistivity value was set to 10 Ωm and extra horizontal grid lines were added to the mesh to decrease the sparsity of resistivity values through the depths comparable to the borehole data. The τ value initially started at 30 which allowed for a model which was very smooth but did not necessarily fit the data very closely. The inversion ran through successive iterations until the RMS error could no longer be reduced at which stage the parameters were decreased and the model run once more. Once the first inversion had been run the apparent resisitivity errors were reduced to 10% the phase errors to 5% and the τ value to 20. The errors and τ were reduced in further inversions until the errors were around 4-5% and the tau value was 10. Once the model

was completed with a low RMS value of between 1-5 and small data errors, a matrix of the resistivity values for each cell was exported from WinGlink.

Data from petroleum well logs were compared to the magnetotelluric surveys. Density data from the Moomba 086 and Mulkurra West 001 boreholes (in the public domain and available on DMITRE's SARIG website (DMITRE 2012)) was input into a porosity/density equation (Davis 1954) to calculate porosity, ϕ:

$$\phi = \frac{\rho_{matrix} - \rho_{\beta}}{\rho_{matrix} - \rho_{\omega}} \tag{5}$$

ρ_{β} is the bulk density of the rock unit these values were taken from the well log data. ρ_{ω} is the density of fluid and according to Champel (2006) can be estimated at ≈ 1.025 g/cm^3. This value is applicable in a temperature range between $50 - 100$ °C (Deighton & Hill 1998). ρ_{matrix} is the matrix density which was assumed to be 2.65 g/cm^3, typical of the sediments in the region (Schon 2011). The well data was sampled with a spatial interval of 15.24 cm for both the Moomba 086 and Mulkurra West 001 well logs. The results showed the need for smoothing filters to be applied to minimise the effects of thin layers of sediments with high porosities. A moving average boxcar filter was calculated using matlab; this average was applied three times with different bin sizes. The bins were 15, 49 and 101 cells wide.

The two petroleum wells were chosen because of their proximity to the magnetotelluric survey sites. The close distance, together with the assumption of one-dimensionality of the strata allowed for a valid comparison of the data. 1-D sections were extracted from the MT surveys at the location of the station closest to the well log at each study location. Archie's law was applied to these sections and used to calculate the porosity at discrete depths. Combining equations (3) and (4) leads to

$$R_t = \alpha \phi^{-m} R_W S_W^{-n} \tag{6}$$

Which can be rearranged for porosity (ϕ) and becomes

$$\phi = 10^{\frac{log\frac{R_W a S_W^{-n}}{R_t}}{m}} \tag{7}$$

Table 1: Summary of parameter value ranges for Archie's law (Equation 7)

parameter	**symbol**	**value range**
Tortuosity	α	2-3 (Salem 2000)
Cementation factor	m	2-3 (Salem & Chilingarian 1999)
Resistivity of Water	(R_W)	0.02-0.09 Ωm (Ucok et al. 1980)
Saturation factor	n	≈ 2 (Khalil & Santos 2009)
Saturation	S_W	0-1

The values applied in this study are given in Table 1.

To ensure that these values have been justly assumed, resistivity tests were carried out on each MT model to determine the effect changing each of these parameters has on the porosity profile. Once the porosity graphs had been produced for both the well log and magnetotelluric data, comparison between the two was required. This was achieved by taking linear regressions of the porosity data from the surveys and finding the difference between the borehole and MT lines for each case study.

OBSERVATIONS AND RESULTS

Case Study 1: Moomba North

The MT model (Figure 4) shows a 2-D resistivity profile of the Moomba North case study. The resistivity values of the upper sediments vary between 1 Ωm and 10 Ωm. The basement is visible at a depth of 3-4 km and has resistivity values between 100 Ωm and 10000 Ωm. The model runs south to north from the left to right sides of the page. From this plot a 1-D resistivity sounding was extracted (Figure 5) which shows a general increase in resistivity until roughly 5 km depth where it starts to decrease. This

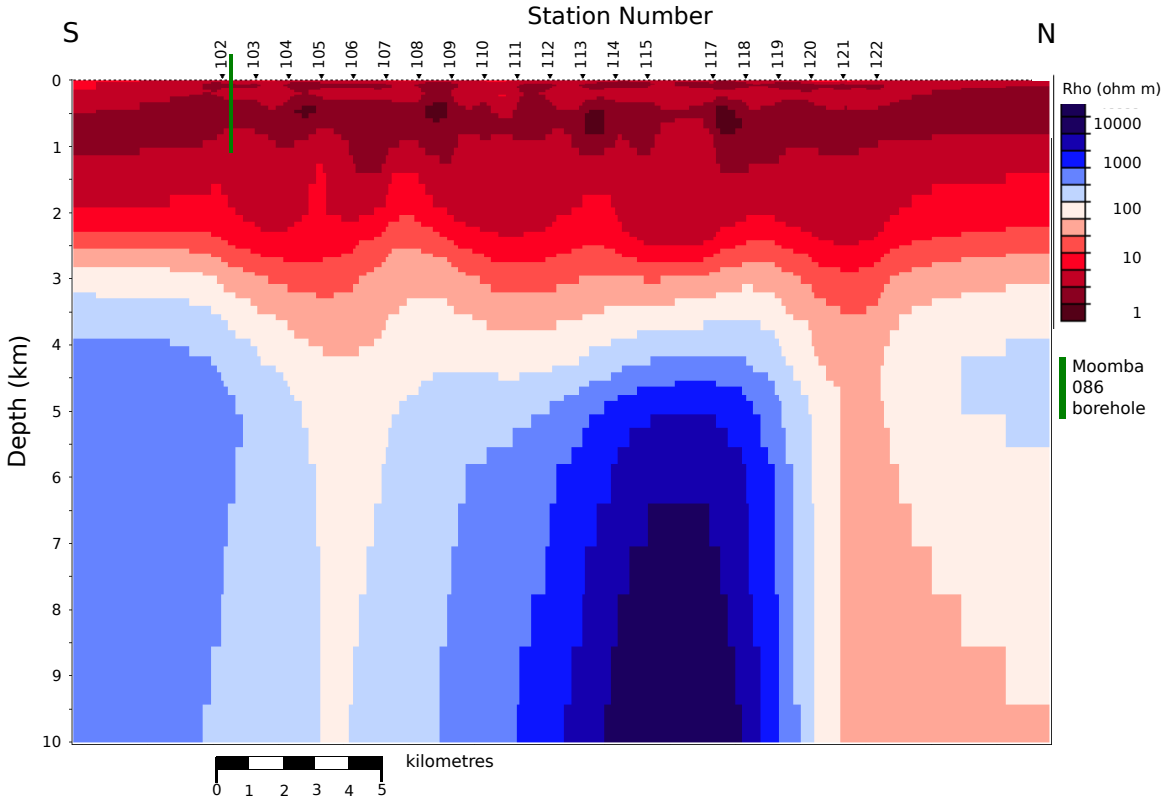

Figure 4: Resistivity profile of the Moomba North magnetotelluric survey (from WinGlink). The colour scale shows the logarithmic resistivity values with blue the most resistive and red the least resistive. The model was produced with three iterative steps. The first set of iterations were made with apparent resistivity errors of 20% phase errors of 10% and a smoothing factor (τ) of 30. The second set of iterations were run with app. res. error = 10% phase error = 5% and τ= 15. The final set of iterations were run with app. res. error = 5% phase error = 3% and $\tau = 7$. Each step was allowed to have a maximum of 30 iterations. The final RMS = 1.1380 . The location of the Moomba 086 borehole is shown in green.

profile was extracted from station 102 as that was the station nearest to the Moomba 086 borehole used to produce the comparable porosity plot (Figure 6). Archie's law was applied to the data using the values shown in Table 2 and the resulting porosity values are shown in Figure 7. Figure 6 (a) shows the porosity values calculated from the density data using Equation 5. $\rho_{matrix} = 2.65$ g/cm^3 and $\rho_\omega = 1.025$ g/cm^3 were assumed as per methods section. Due to the high sampling rate of 6.65 points per metre a moving average boxcar filter was applied to minimise the effects of thin layers. The results of

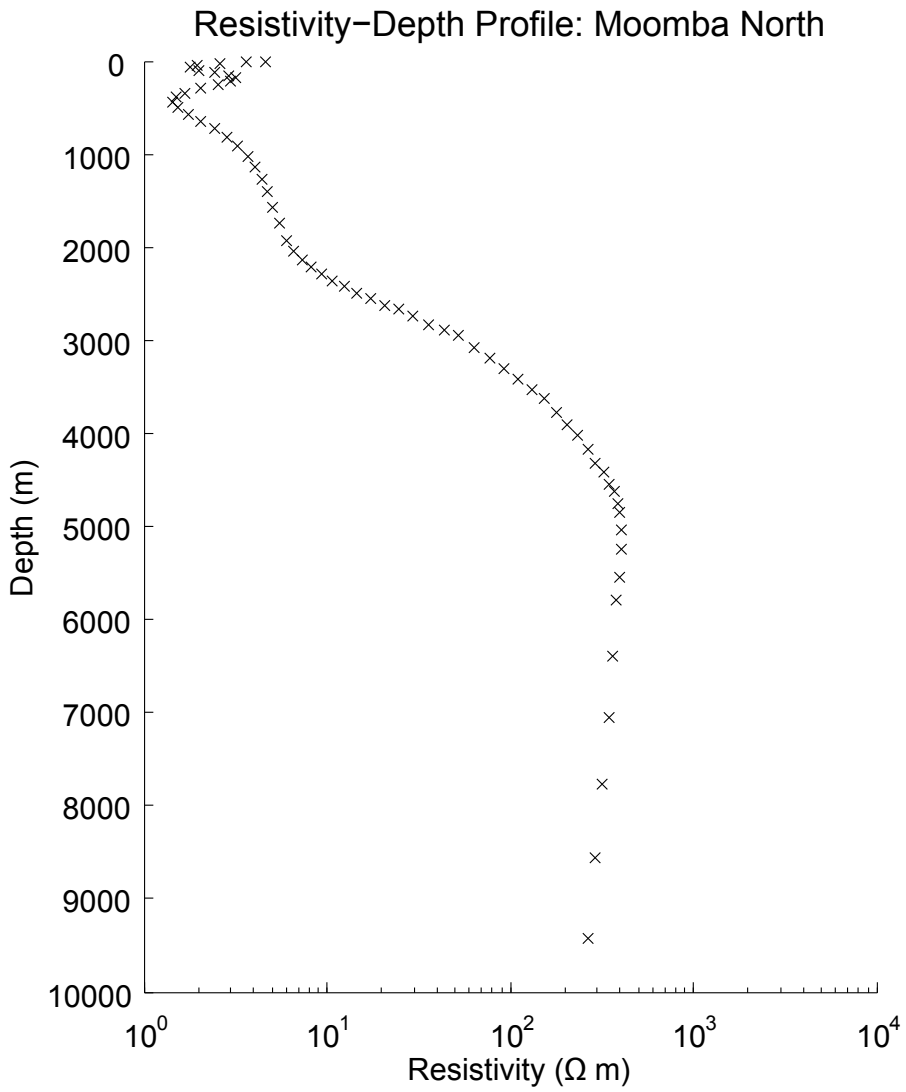

Figure 5: Resistivity at the Moomba North MT survey case study station 102. The resistivity values are shown on a logarithmic scale. Values were extracted from the WinGlink model and plotted using matlab. These values are used to produce porosity values using Archie's law

this are shown in Figure 6 each of the filters can be seen to reduce the number and size of the peaks present in plot a) to a progressively greater extent.

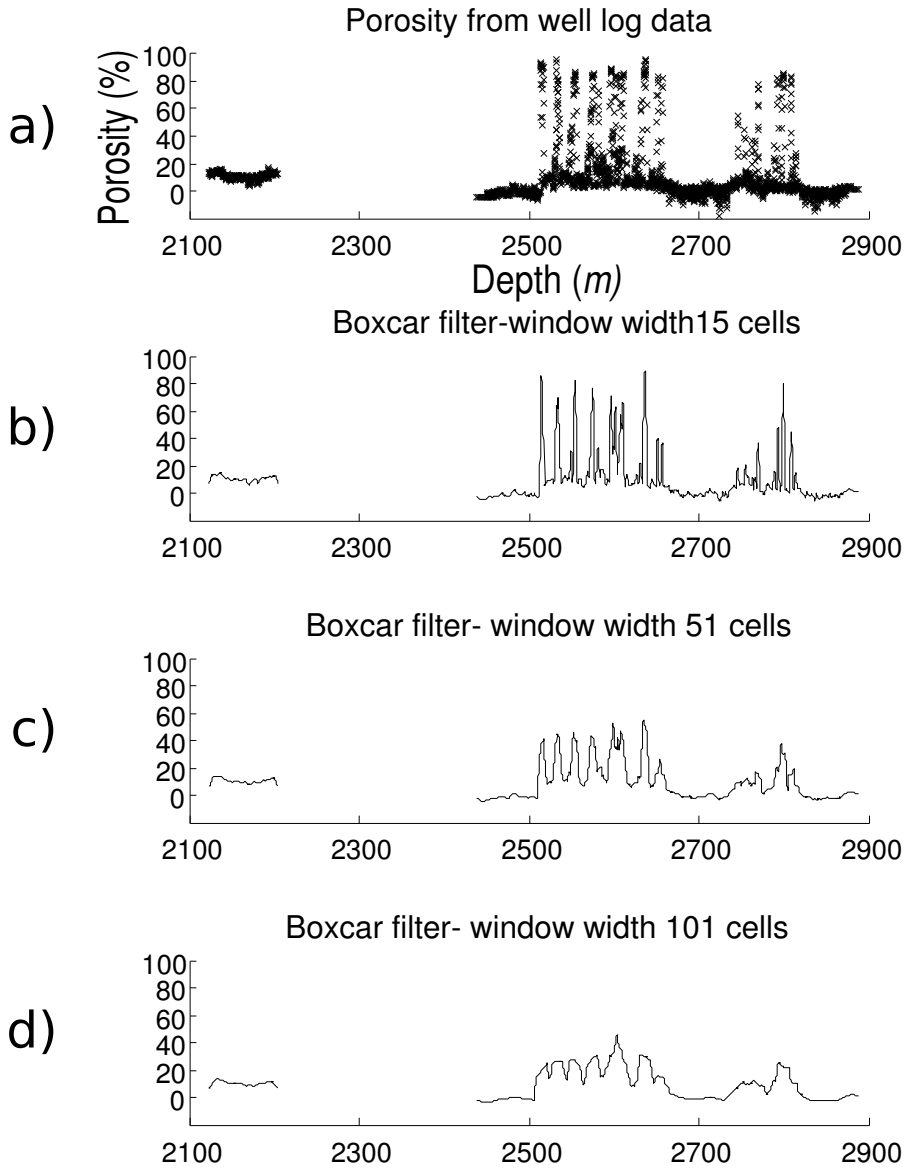

Figure 6: Porosity depth profile from borehole data at the Moomba 86 well site.
a) porosity plot inferred from density profile c.f. Equation (5).
b) moving average boxcar filter applied to (a) with a bin size of 15 cells.
c) moving average boxcar filter applied to (a) with bin size of 49 cells.
d) moving average boxcar filter applied to (a) with bin size 101 cells.
Note that no data was available between 2220 and 2430 m.

Case Study 2: Mungerannie

The resistivity values shown in the 2-D model (Figure 8) vary between 1 Ωm and 10 Ωm for the upper sediments. The basement rocks start between 1-2 km depth and have

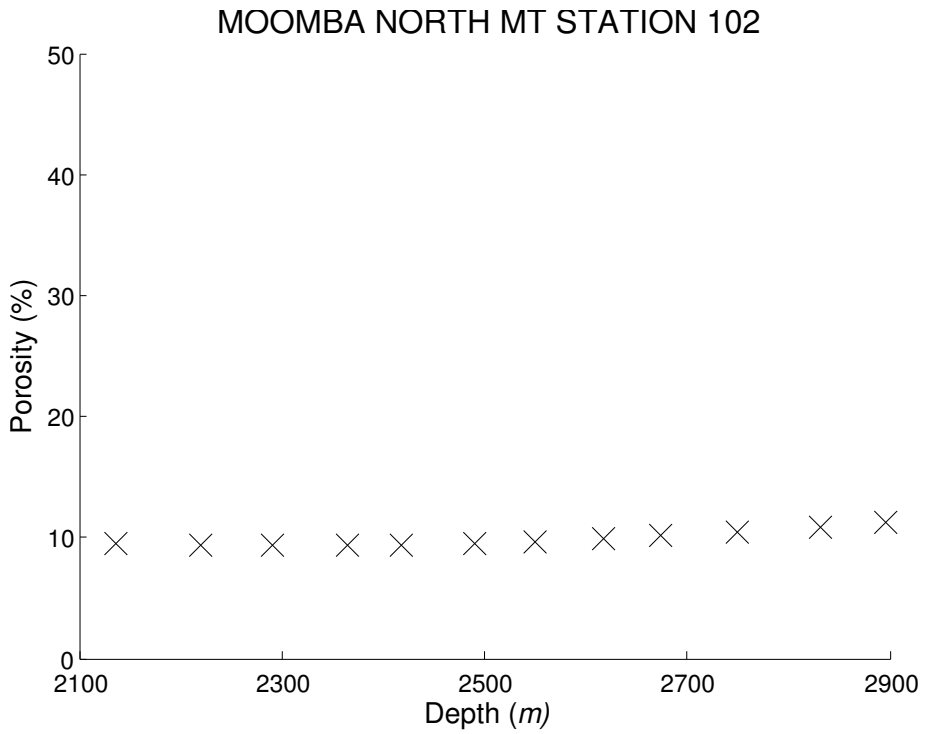

Figure 7: Porosity at the Moomba North MT survey station 102. Station 102 is the closest site in the survey to the Moomba 086 borehole. The porosity was calculated using Archie's law and the values are very stable, and the values follow a linear trend showing only a 0.05% change through the depth range. The depth shown ranges from 2000 to 3000 m as this is the logged depth of the borehole.

Table 2: Values for Archie's law used in Equation 7 to produce the Moomba North 1-D porosity profile.

Parameter	**Value**
R_W	0.02
S_W	0.3
α	3
n	2
m	2.8

resistivity values of 100-10000 Ωm. The model runs from north to south from left to right. A 1-D resistivity sounding (Figure 9) was extracted from this model. It shows an increase in resistivity down to 3 km at which stage the resistivity decreases. This profile was extracted from station 116 as it was the closest to the Mulkurra West 001 borehole. Archie's law (Equation 7) was applied to the data using the values shown in Table 3

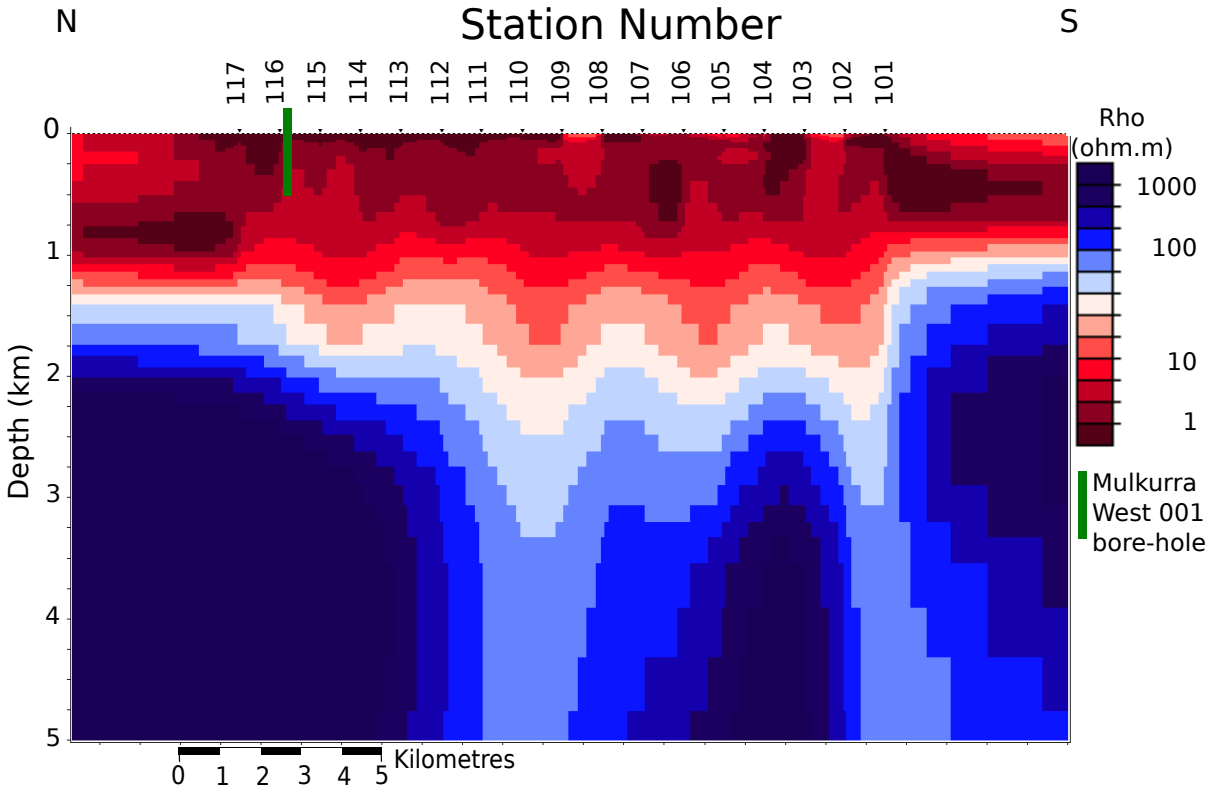

Figure 8: The resistivity profile of the Mungerannie magnetotelluric survey (from WinGlink). The colour scale shows the logarithmic resistivity values with blue the most resistive and red the least resistive. The model was produced with three iterative steps. The first set of iterations were made with apparent resistivity errors of 20% phase errors of 10% and a smoothing factor (τ) of 30. The second set of iterations were run with app. res. error = 10% phase error = 5% and τ= 15. The final set of iterations were run with app. res. error = 5% phase error = 3% and τ = 7. Each step was allowed to have a maximum of 300 iterations. The final RMS = 2.2033. The location of the Mulkurra West 001 borehole is shown in green.

and the resulting porosity values are shown in Figure 10. Figure 11 shows the porosity values calculated from the density data using Equation 5. ρ_{matrix} = 2.65 g/cm^3 and ρ_ω = 1.025 g/cm^3 were assumed as per methods section. A boxcar filter was applied to minimise the effect of thin layers. The effects of thin layer were less pronounced in this case study than in the Moomba North case study and thus the smoothing filter had a smaller effect.

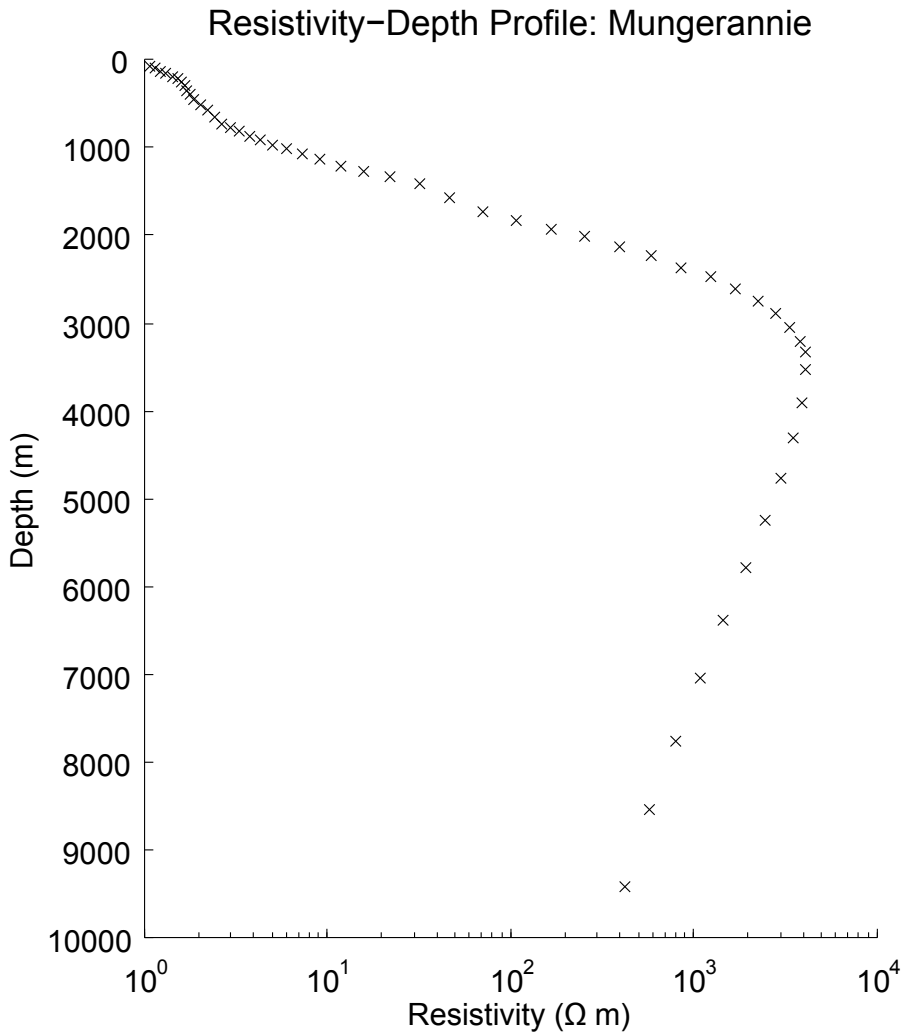

Figure 9: Resistivity section of the Mungerannie MT survey from station 116. The resistivity axis has a logarithmic scale. The values were taken from the WinGlink model and plotted using matlab. The values are used to produce a porosity plot using Archie's law (Equation 7).

Table 3: Values for Archie's law used in Equation 7 to produce the Mungerannie 1-D porosity profile

Parameter	**Value**
R_W	0.08
S_W	0.2
α	3
n	2
m	2.8

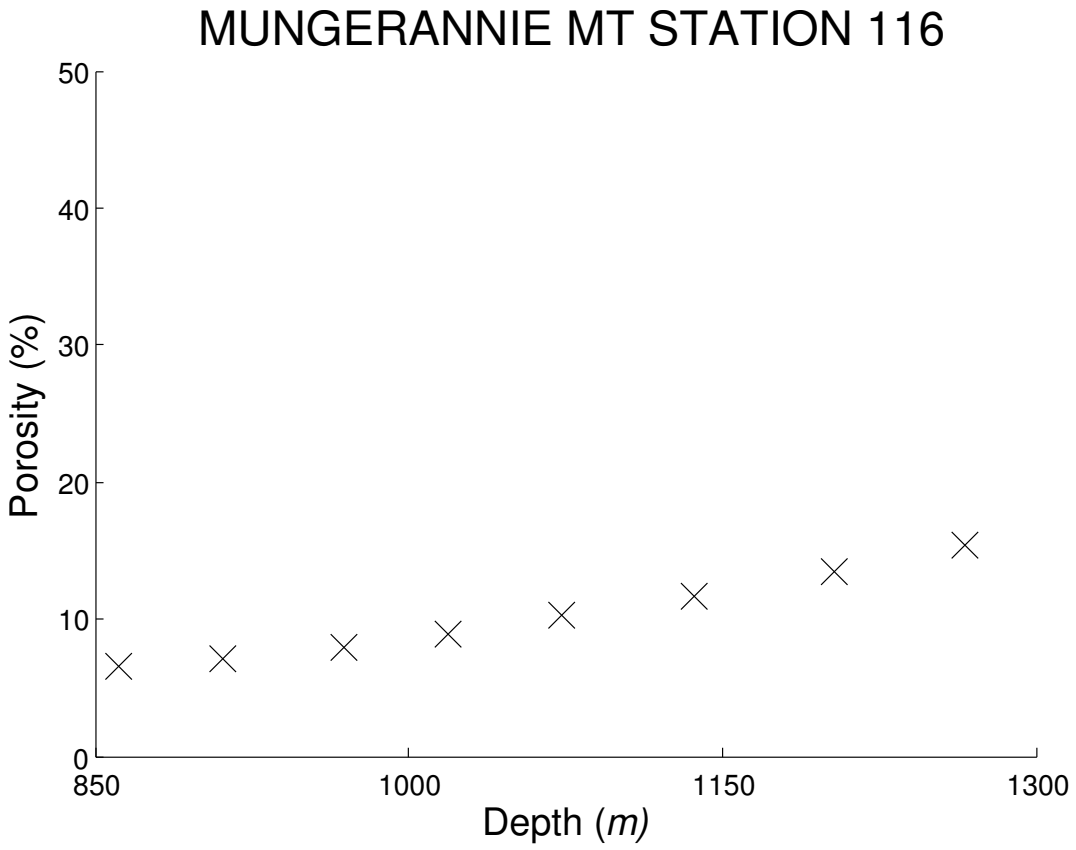

Figure 10: Porosity at the Mungerannie magnetotelluric survey station 116. Station 116 is the closest site in the survey to the Mulkurra West 001 borehole. The porosity was calculated from resistivity values using Archie's law and the values show a slightly convex up curve, with a variation of around 1% through the depth range. The depth shown ranges from 850 to 1300 m as this is the logged depth of the borehole.

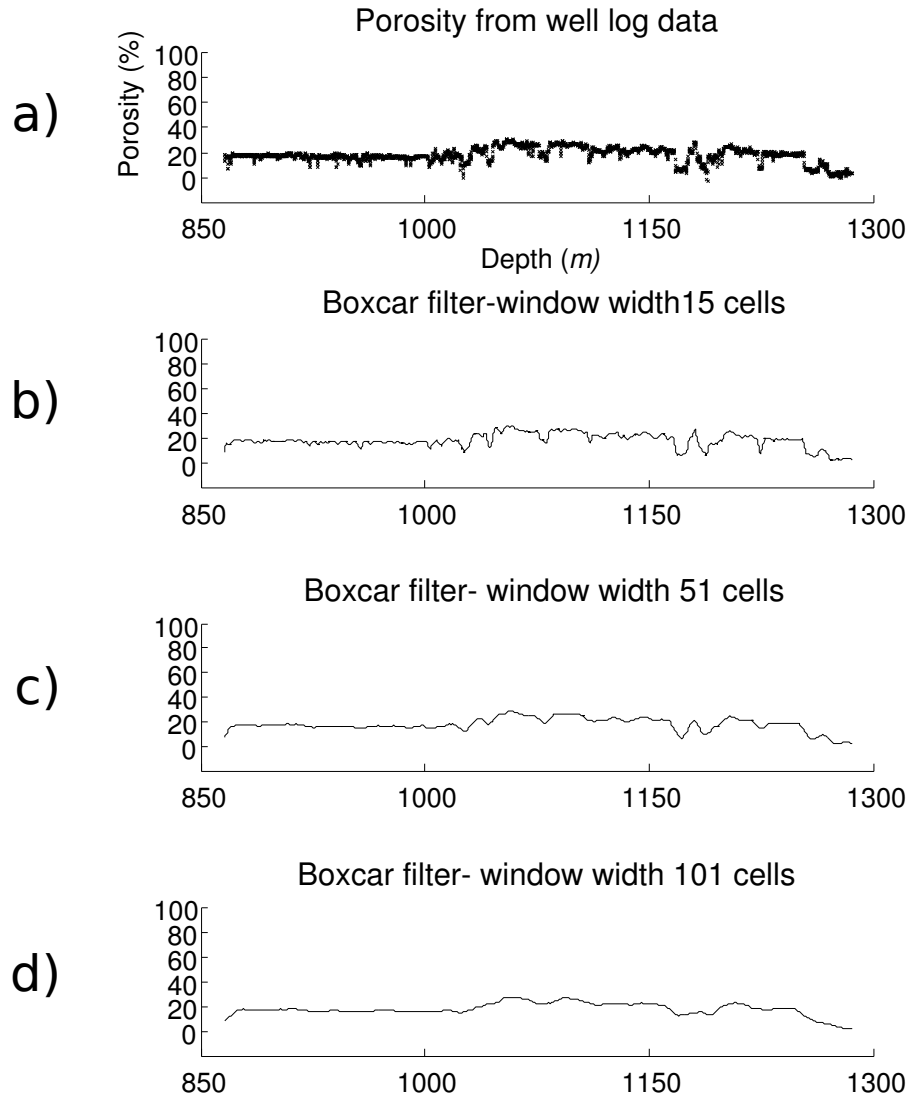

Figure 11: Porosity depth profile from borehole data at the Mulkurra West 001 well site.
a) porosity plot inferred from density profile c.f. Equation (5).
b) moving average boxcar filter applied to (a) with a bin size of 15 cells.
c) moving average boxcar filter applied to (a) with bin size of 49 cells.
d) moving average boxcar filter applied to (a) with bin size 101 The purpose of the filters was to reduce the effect of small conducting layers within the rock unit.

DISCUSSION

Case Study 1: Moomba North

To a depth of ≈ 5 km the resistivity profile (Figure 4) shows a general trend of increasing resisitivity with depth. This is to be expected in a roughly one-dimensional (i.e. similar in all horizontal directions) sedimentary basin. After 5 km the basement rocks are present and due to compositional and temperature changes these rocks begin to have lower resistivities. The increasing resisitivity of the first 5 km is most likely caused by the effect of compaction reducing the porosity (Smith 1971);

$$\phi_z = \phi_T e^{-bz} \tag{8}$$

where

ϕ_z is porosity at depth z

ϕ_T is porosity at the surface

$-b = 0.0014$ /m (constant)

z is depth in metres.

This in turn reduces the permeability leading to increasingly poor conduction of fluids and thus electric currents. The porosity depth plot (Figure 7) does not show this relationship. Archie's law is only valid in sedimentary settings and thus when it is applied to the whole profile; which includes basement rocks, it fails. This leads to erroneous porosity values within the deeper sections of the profile near the intersection with basement rocks. See Appendix B for the porosity curve from 0-10 km. It is possible this basement rock has some effect on the profile in Figure 7.

Within the borehole porosity data (Figure 6) portions of the plot give negative values, these are a product of data processing and can be changed by altering the variables in Equation 5. Changing these values increases the porosity across the whole curve such that some data points become greater than 100%. This is not possible and thus a compromise must be made for the values in order to achieve data which best represents feasible values. In Figure 6 (a) the thin peaks make it hard to find a compromise of values between 0 and 100%. These peaks have been interpreted as beds of more porous sediments and not artefacts of data processing. The peaks do not show up on the resistivity-derived ϕ plot (Figure 7) due to the lower spatial density of points across the 2100-2900 m depth. To counter this, the moving average boxcar filter was applied to the borehole porosity data (Figure 6). It is easier to see the differences between the smoothed data (plot (d)) and the MT porosity plot.

Table 4: Mean and standard deviation data for the magnetotelluric and borehole surveys in the Moomba North case study

Data set	**Average porosity (%)**	**Standard deviation**
Moomba 086 unfiltered data	9.55	19.16
Moomba 086 filtered (window width 101 cells)	9.47	10.76
Moomba North MT data	9.89	0.655

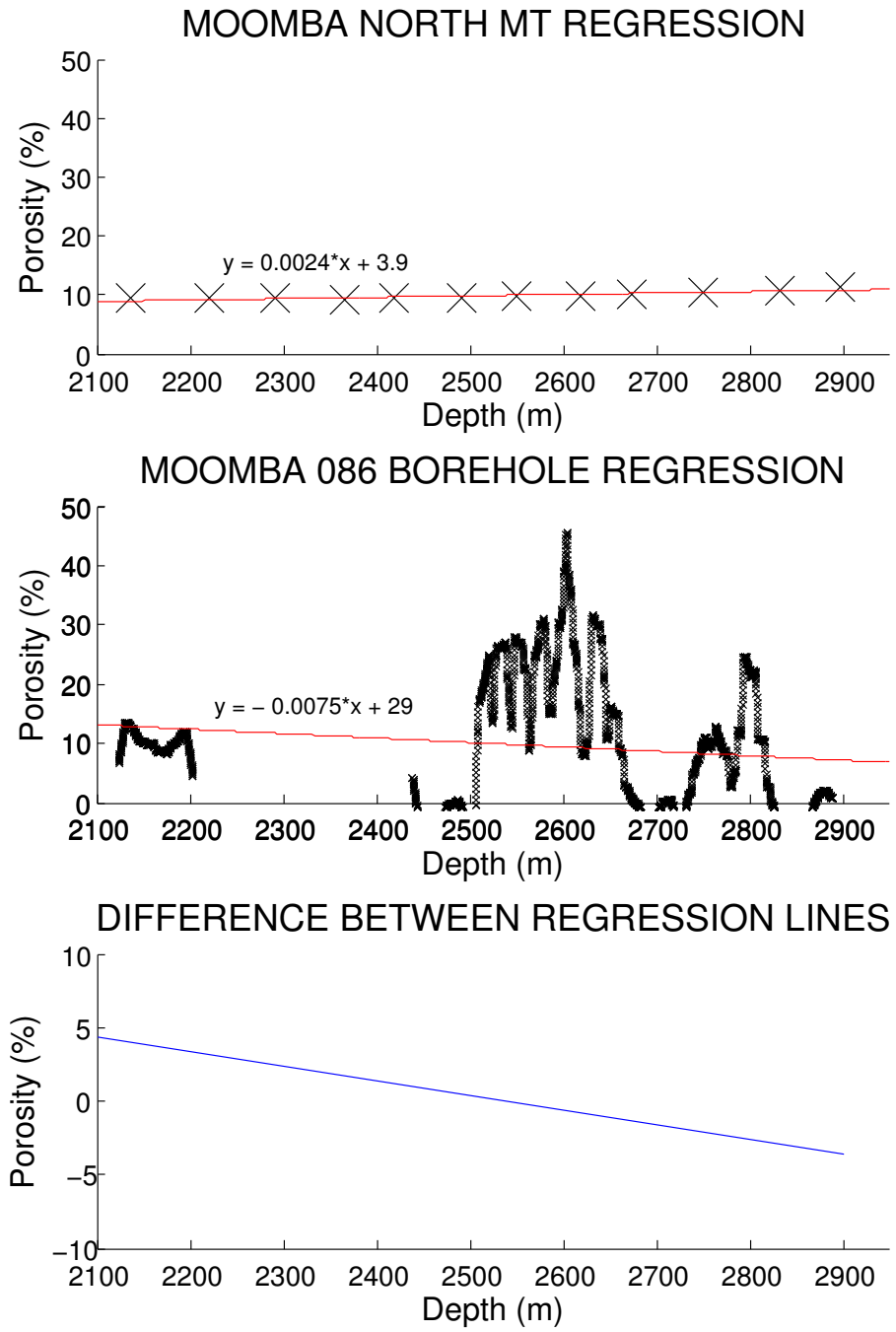

Figure 12: Moomba North porosity data with a linear regression (performed on matlab). (a) MT-derived data $r^2 = 0.7892$. (b) Borehole-derived data, the regression was performed on the data set which had undergone a moving average boxcar filter with a bin size of 101 cells; $r^2 = 0.227$. (c) The difference between the two regression lines, produced by taking the difference of the two regression lines at 100 m intervals and plotting the line encompassing these values.

Table 5: Linear regression statistics for the Moomba North case study. The borehole statistics were calculated on the data set which had a moving average boxcar filter applied with a bin width of 101 cells.

Data set	**slope**	**y-intercept**	$\mathbf{R}^2$
Moomba North MT	0.0024	3.9	0.7892
Moomba 086 borehole	-0.0075	29	0.0227

A basic statistical examination of the Moomba North data in Table 4 shows that, as expected the borehole derived data shows a much greater deviation from the mean than the MT derived data. A linear regression was performed on both the MT- and borehole-derived porosity data sets. Although the MT-derived data is not linear, it is approximately so for the comparable depths of 2100-2900 m. The results of these regressions are shown in Table 5 and the plots in Figure 12. Plot (a) shows a linear regression of the MT-derived porosity data, this data appears to fit the regression line quite well and $R^2 = 0.7892$ (Table 5). Plot (b) shows the linear regression for the borehole-derived porosity data. The regression was performed on the data set from Figure 6 plot (d) and thus was smoother than the raw data. The data is not very linear; for the purposes of this study that was not important as only an average of the data was required. For this reason the $R^2 = 0.0227$ is not important. The most important part was to get a linear approximation across the depth to compare to the MT-derived data. Plot (d) (Figure 5) shows the difference between the two linear regression lines. This plot was created by calculating the porosity values for each line at 100 m depth intervals from 2100 m to 2900 m. The MT porosity values were subtracted from the borehole values and the resulting points were plotted as a line. This line shows that the linear approximations of the MT and borehole data sets differ by less than 5% porosity between 2100 m and 2900 m.

Changing the variables used in producing the porosity plots created changes in the curves which in turn caused changes in the correlation between the two data sets. Figure 13 shows the effect changing the variables in Archie's law (eq. 7) has on the estimated

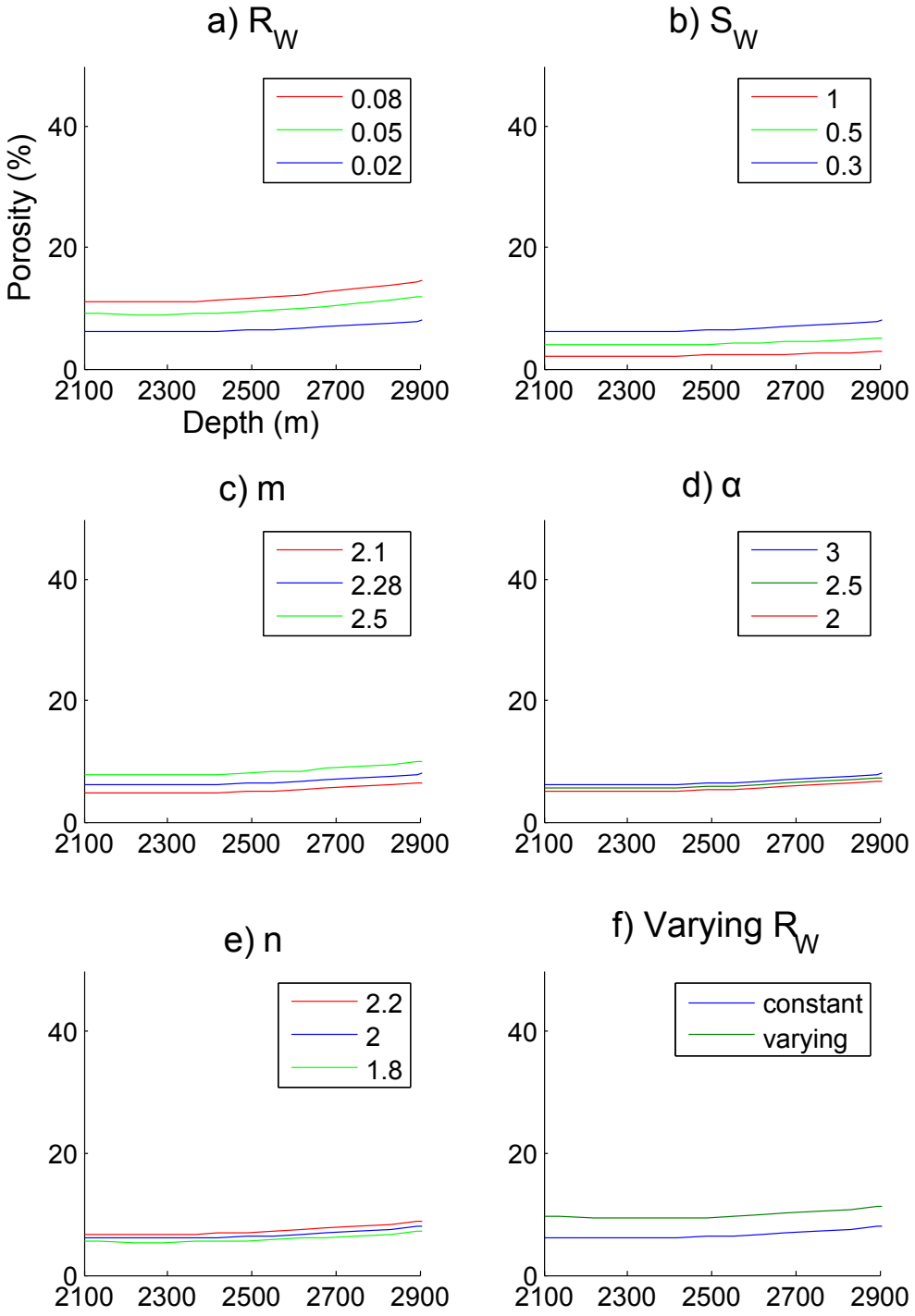

Figure 13: The effects of changing the variables in Archie's Law on the calculated porosity for the Moomba North case study. The blue line represents a standard to which the others are compared: $R_W = 0.02$; $\alpha = 3$; $S_W = 0.3$; n=2; m=2.28. Plot A: changing the resisitivity of water, R_W. Plot B: changing the water saturation. Plot C: changing the cementation exponent. Plot D: changing the tortuosity (α). Plot E: changing the saturation exponent, n. Plot F: the standard compared to a profile with a changing R_W from 0.08 to 0.0190 decreasing by 0.001 increments.

porosity. Values were changed for R_W, α, S_W, n and m in order to determine the effects this had on porosity values. Figure 13 shows that a reduction in R_W linearly decreases the porosity values; if the water is less resistive (eg due to a temperature increase) it can account for a larger portion of the conductivity of the unit and thus to maintain the bulk resistivity the porosity must decrease. Reducing S_W increases the calculated porosity because Archie's law assumes that water will conduct the electromagnetic waves and thus in order for the resistivity to remain constant with a lower percentage of water the rock must be more porous to allow the waves to travel through at the same rate. As the S_W is raised to the power of n (Equation 7) it has an exponential effect on the porosity values. A reduction in m linearly reduces the porosity, because as the sediments are less cemented less porosity is required to maintain the resistivity. As α is reduced it in turn reduces the porosity. If the tortuosity of the path increased larger pores and more pore space would be required in order to maintain the same resistivity.

The final plot in Figure 13 shows the effect of changing R_w throughout the depth of the plot. In this case the values started at 0.08 and linearly decreased to 0.02 Ωm. Although the difference is not great, it has the effect of slightly changing the shape of the line. The two lines are closer together at 2900 m than they are at 2100 m. The values of R_W need to vary throughout the length of the plot as they are not constant in strata. As depth and temperature increase the resistivity of water decreases (Hersir & Arnason 2009).

Case Study 2: Mungerannie

To a depth of $\approx$ 3 km the resistivity profile (Figure 8) shows a general trend of increasing resistivity with depth. Beyond this depth the resistivity starts to decrease (Figure 9). The initial increase in resistivity is cause by compression, defined by Equation 8. Within the borehole porosity data (Figure 11) portions of the plot give negative porosity values.

As in the Moomba North data this is a function of data processing and the effect was minimised by altering the variable values. A moving average boxcar filter was applied to this data in an attempt to make the data more linear and thus easier to compare to the MT data. The results of the applied filter are shown in plots (b), (c) and (d) of Figure 11, the filters were produced the same way as outlined in case study 1.

Table 6: Mean and standard deviation data for the magnetotelluric and borehole surveys in the Mungerannie case study

Data set	**Average porosity (%)**	**Standard deviation**
Mulkurra West 001 unfiltered data	17.74	6.07
Mulkurra West 001 filtered (window width 101 cells)	17.66	5.06
Mungerannie MT data	10.2	3.1578

A basic statistical analysis of the Mungerannie data, shown in Table 6 shows that the borehole data has a higher mean and larger standard deviation than the MT derived data. A linear regression was performed on both the MT- and borehole-derived porosity data sets. The MT-derived data was approximately linear for the comparison depth of 850 m to 1300 m and thus the line fit well, with an $R^2 = 0.9834$ (Figure 14). The borehole derived data was harder to fit to a linear regression. A moving average was applied in an attempt to achieve a smoother line. The fit was not as good as that of the MT-derived data (Figure 14). The lack of linearity in the borehole derived data ensured a low R^2 value ($R^2 = 0.0212$). This low value is unimportant as all that was required was a linear approximation for the data over the 850 to 1300 m depth. The results from the two regressions are summarised in Table 7. Figure 14 shows the difference of the

Table 7: Linear regression statistics for the Mungerannie case study. The borehole statistics were calculated on the data set which had a moving average boxcar filter applied with a bin width of 101 cells.

Data set	**slope**	**y-intercept**	**R^2**
Mungerannie MT	0.018	-10	0.9834
Mulkurra West 001 borehole	-0.061	24	0.0212

two linear regression lines, it was created by calculating the porosity values for each line at 100 m intervals from 850 to 1300 m. The MT porosity values were subtracted from the borehole values and the resulting points were plotted as a line. This line shows the linear approximations of the MT and borehole data sets differ by less than 15% porosity, with a smaller difference in values at the deeper section of the plot.

A similar investigation, as was carried out in case study 1, was conducted regarding the effects of changing the variables of Archie's law (Equation 7) on the estimates of porosity. The general trend results are the same for this case study as for the Moomba North study; pertinent results to notice are the effect which varying the value of R_W has on the shape of the curve and that a reduction in S_W not only increases the porosity but changes the shape of the curve.

Permeability

Once the porosity values from the MT and density data sets had been correlated over the investigation depths, the results could be used to extrapolate the MT porosity values over a larger depth to encompass the whole of the geothermally prospective depth. This would give a good indication of the prospectivity of the region. It does not however dismiss the fact that the purpose of this study was to show that MT can be used as a primary inexpensive exploration method. In order for this to be the case the estimated parameters for Archie's law suggested in table 1 can be used. In South Australia many of the regions being explored for geothermal potential have previously been explored for petroleum, because of this there have been many boreholes drilled which have had logging undertaken for the length of the well. Provided the site are no longer active the results from these surveys are often in the public domain and can be used to determine the variables required for Archie's law to be accurate.

In order to improve the comparison between the magnetotelluric and petroleum well based results further investigation could be undertaken on the resistivity surveys taken on the petroleum well logs. These could be used to further correlate the data and provide a link between the resistivity data from the magnetotelluric survey and the density data of the petroleum well logs.

The estimation of porosity is only a step towards understanding the ways in which these surveys can determine the permeability of geothermal reservoirs. Once the porosity values for the petroleum wells and magnetotelluric surveys have a good correlation they can be used to estimate the permeability. Examples of how this can be achieved include Leary & Al-Kindy (2002) and Chilingar et al. (1963) who have both produced a logarithmic relationship between porosity and permeability, where $K = 10^{\phi}$. Figures 16 and 17 show examples of permeability plots calculated from the porosity data of the Moomba North and Mungerannie MT surveys. In order to further investigate the ability of magnetotellurics to determine permeability a control must be devised such that calculated values can be compared to values known to be correct.

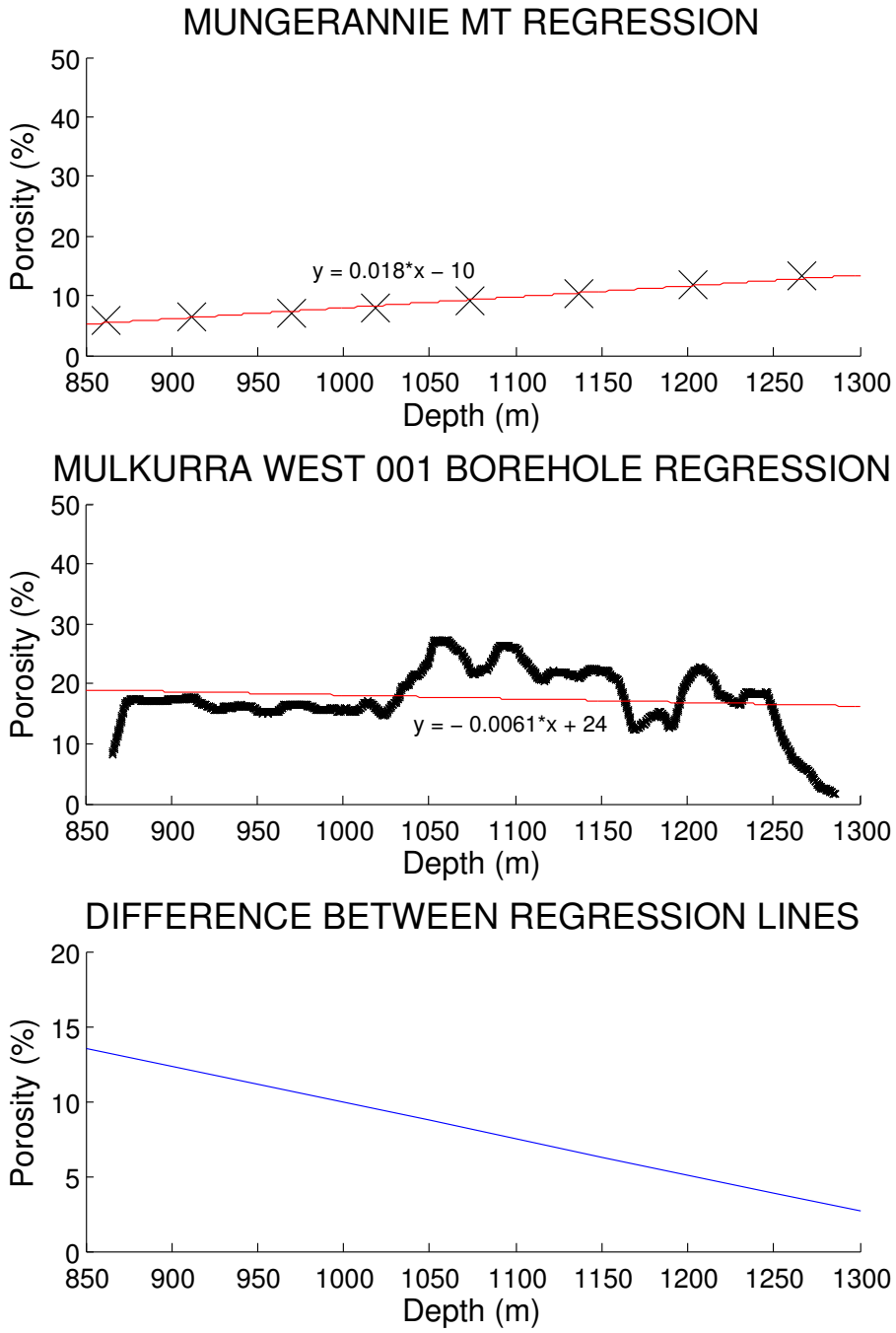

Figure 14: Mungerannie MT-derived porosity data with a linear regression (performed on matlab). (a) MT-derived data, $R^2 = 0.9834$. (b) Borehole-derived data, the regression was performed on the data set which had undergone a moving average boxcar filter with a bin size of 101 cells; $R^2 = 0.0212$. (c) The difference between the two regression lines; produced by taking the difference of the two regression lines at 100 m intervals between 850 and 1300 m and plotting the line encompassing these values.

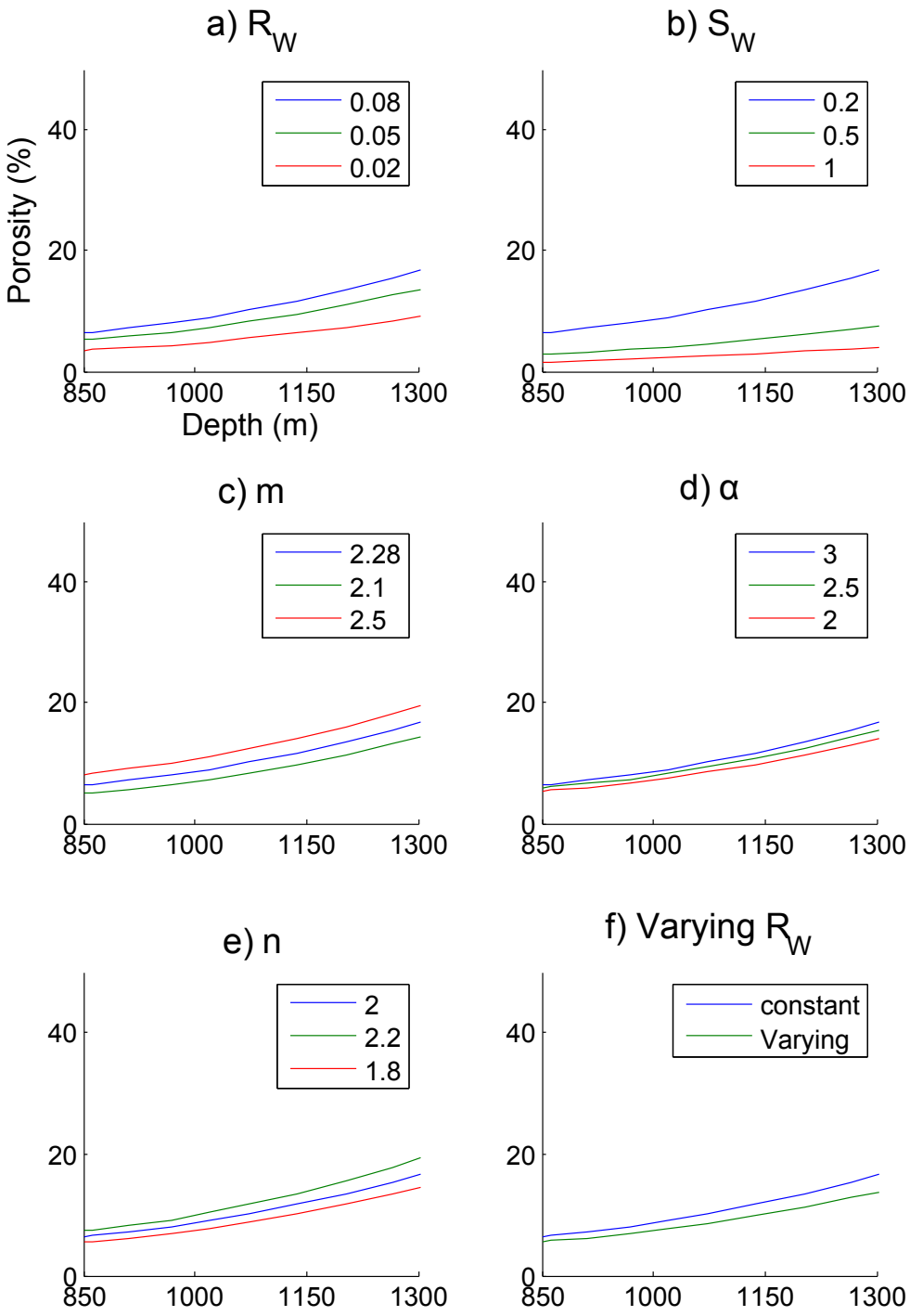

Figure 15: The effect of changing the variables in Archie's Law on calculated porosity in the Mungerannie survey. The blue line represents a standard to which the others are compared: $R_W = 0.08$; $\alpha = 3$; $S_W = 0.2$; n=2; m=2.28. Plot A: changing the resistivity of water, R_W. Plot B: changing the water saturation. Plot C: changing the cementation exponent. Plot D: changing the tortuosity, α. Plot E: changing the saturation exponent, n. Plot F: the standard compared to a profile with a changing R_W from 0.08 to 0.024 decreasing by 0.001 increments.

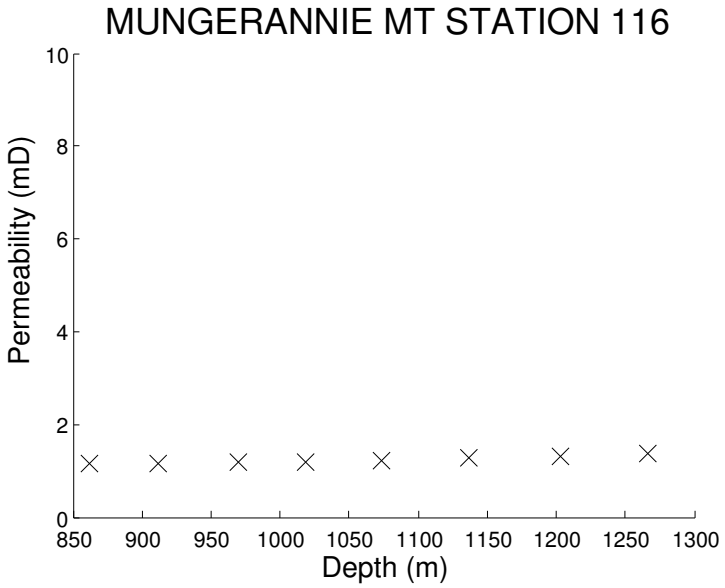

Figure 16: Estimation of permeability of the Moomba North case study using porosity calculated with Archie's law and an exponential relationship between porosity and permeability.

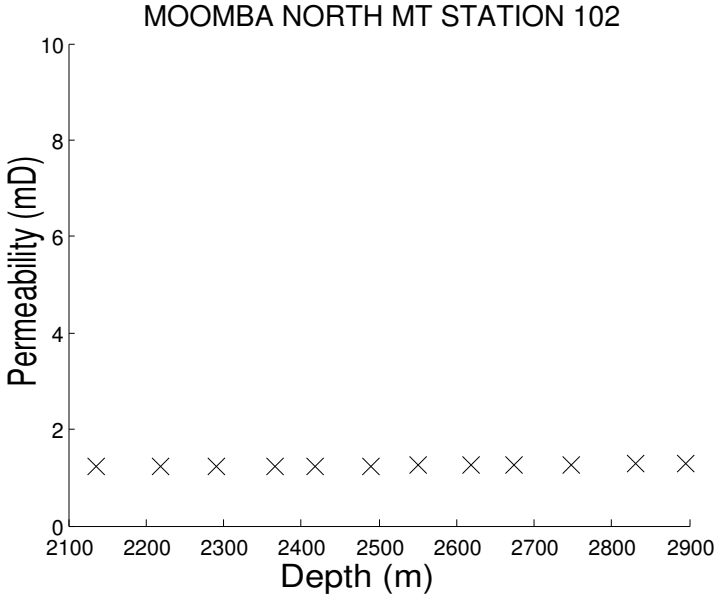

Figure 17: Estimation of permeability of the Mungerannie case study using porosity calculated with Archie's law and an exponential relationship between porosity and permeability.

CONCLUSIONS

As the world looks towards sustainable means of energy production the importance of geothermal energy becomes increasingly clear. As more exploration is carried out to search for geothermally prospective areas companies wish to know that they are receiving the best knowledge about these areas and can carry out drilling programs with minimal risk. To this end an understanding of the role magnetotellurics can play in understanding the petrophysics of an area is imperative. A solid understanding of the way in which porosity is shown in a resistivity survey will minimise risk by showing one of the features which determines the prospectivity of a region. By comparing magnetotelluric derived porosity with that derived from petroleum boreholes this investigation has demonstrated the reliability of magnetotellurics determining porosity. It has also provided a base for further investigation into the ways in which MT can be used to accurately determine permeability.

ACKNOWLEDGMENTS

I would like to thank my supervisor Stephan Thiel for all his help throughout the year; Lars Krieger for invaluable technical support and Tania Dhu and the geophysicists at DMITRE. Thanks also to Sebastian Schnaidt and to my fellow honours students Paul Soeffky and Kelly Sharrad for moral and editing support.

REFERENCES

Archie, G. E. (1942). The electrical resistivity log as an aid in determining some reservoir characteristics., *Petroleum Transactions of AIME* **146**: 54–62.

Bedrosian, P. A. (2007). Mt+, integrating magnetotellurics to determine earth structure, physical state and processes, *Surveys in geophysics* **28**: 121–167.

Berryman, J. G. (2003). Electrokinetic effects and fluid permeability, *Physica B* **338**: 270–273.

Champel, B. (2006). Discrepancies in brine density databases at geothermal conditions, *Geothermics* **35**: 600–606.

Chilingar, G. V., Main, R. & Sinnokrot, A. (1963). Relationship between porosity, permeability and surface areas of sediments, *Journal of Sedimentary Petrology* **33**: 759–765.

Davis, D. (1954). Estimating porosity of sedimentary rocks from bulk density, *The Journal of geology* **62**: 102–107.

Deighton, I. & Hill, A. (1998). *Volume 4 Cooper Basin*, PIRSA, chapter 9: Thermal and Burial History, pp. 143–156.

DMITRE (2012). https://sarig.pir.sa.gov.au/Map.

Glover, P. (2010). A generalized archies law for n phases, *Geophysics* **75**(6): E247–E265.

Heise, W., Caldwell, T., Bibby, H. & Bannister, S. (2008). Three dimensional modelling of magnetotelluric data from the rotokawa geothermal field, taupo volcanic zone, new zealand, *Geophysics Journal International* **173**: 740–750.

Hersir, G. P. & Arnason, K. (eds) (2009). *Resistivity of rocks*, UNU-GTP and LaGeo, Geothermal Training Program. Short Course on SUrface Exploration for Geothermal Resources.

Khalil, M. & Santos, A. (2009). Influence of degree of saturation in the electric resistivity-hydraulic conductivity relationship, *Surveys in geophysics* **30**: 601–615.

Leary, P. & Al-Kindy, F. (2002). Power-law scaling of spatially correlated porosity and log(permeability) sequences from north-central north sea brae oilfield well core, *Geophysics J. Int* **148**: 426–422.

Ledru, P. & Frottier, L. (2010). *Geothermal Energy Systems; Exploration, Development and usilization*, Wiley-VCH.

Mackie, W. R. R. (2001). Nonlinear conjugate gradients algorithm for 2-d magnetotelluric inversion, *Geophysics* **66**(1): 174–187.

Meju, M. (2002). Geoelectromagnetic exploration for natural resources: Models, case studies and challenges, *Surveys in geophysics* **23**: 133–205.

Neumann, N., Sandiford, M. & Foden, J. (2000). Regional geochemistry and continental heat flow: inplications for the origin of the south australian heat flow anomaly, *Earth and Planetary Science Letters* **183**: 107–120.

Salem, H. (2000). Interralationships among water saturation, permeability and torsuosity for shaly sandstone reservoirs in the atlantic ocean, *Energy Sources* **22**: 333–345.

Salem, H. & Chilingarian, G. (1999). The cementation factor of archie's equation for shaly sandstone reservoirs, *Petroleum Science and Engineering* **23**: 83–93.

Schon, J. H. (2011). *Handbook of Petroleum Exploration and Production*, Vol. 8, Elsevier, chapter 4 Density, pp. 97 – 105.

Sheriff, R. E. (2002). *Encyclopedic Dictionary of Applied Geophysics*, Vol. 13, 4 edn, Society of Exploration Geophysicists.

Simpson, F. & Bahr, K. (2005). *Practical Magnetotellurics*, Cambridge University Press.

Smith, J. (1971). The dynamics of shale compaction and evolution of pore-fluid pressures, *Mathematical geology* **3**: 239–263.

Spichak, V. & Manzella, A. (2009). Electromagnetic sounding of geothermal zones, *Journal of Applied Geophysics* **68**: 459–478.

Stockill, J. (2008). 2008 cooper mt survey operations report.

Ucok, H., Ershaghi, I. & Olhoeft, G. (1980). Electrical resistivity of geothermal brines, *Journal of Petroleum Technology* **32**: 717–727.

APPENDIX A: ADDITIONAL INFORMATION – PART I

Table 8: Locations of MT stations for the Mungerannie survey, locations exported from DMITRE's SARIG website (DMITRE 2012). The survey was conducted in February 2008 and all UTM co-ordinates are in zone 54.

Station Number	UTM Northing	UTM Easting	Longitude	Latitude
101	6901289.92	271855.57	138.680117	-27.994033
102	6902294.08	271805.28	138.6798	-27.984967
103	6903289.33	271765	138.679583	-27.975983
104	6904287.79	271706.65	138.679183	-27.966967
105	6905290.27	271661.41	138.678917	-27.957917
106	6906287.14	271612.94	138.678617	-27.948917
107	6907293.75	271587.22	138.67855	-27.939833
108	6908288.24	271512.5	138.677983	-27.93085
109	6909287.08	271468.91	138.677733	-27.921833
110	6910267.26	271417.51	138.6774	-27.912983
111	6911285.58	271330.91	138.676717	-27.903783
112	6912264.78	271327.09	138.676867	-27.89495
113	6913265.17	271271.96	138.6765	-27.885917
114	6914262	271221.81	138.676183	-27.876917
115	6915260.69	271170.06	138.67585	-27.8679
116	6916261.21	271121.52	138.67555	-27.858867
117	6917259.89	271069.76	138.675217	-27.84985

Table 9: Locations of MT stations for the Moomba North survey, locations exported from DMITRE's SARIG website (DMITRE 2012). The survey was conducted in February 2008 and all UTM co-ordinates are in zone 54.

Survey Line	Station Number	UTM Northing	UTM Easting	Longitude	Latitude
1	1	6899978.11	427986.69	140.267433	-28.0235
1	2	6900997.41	428000.23	140.267633	-28.0143
1	3	6902003.68	428004.03	140.267733	-28.005217
1	4	6902997.04	427995.9	140.267711	-27.99625
1	5	6903995.95	427992.07	140.267733	-27.987233
1	6	6904994.83	428000.83	140.267883	-27.978217
1	7	6905998.99	428003.08	140.267967	-27.969153
1	8	6907000.02	428000.03	140.267997	-27.960117
1	9	6907998.94	427998.97	140.268047	-27.9511
1	10	6909001.89	428003.1	140.26815	-27.942047
1	11	6910000.15	428002.04	140.2682	-27.933036
1	12	6911008.69	428015.69	140.2684	-27.923933
1	13	6912001.89	428002.96	140.268331	-27.914967
1	14	6913001.13	427999.15	140.268353	-27.905947
1	15	6914996.99	428000.02	140.268483	-27.887931
1	16	6915999.36	428000.63	140.26855	-27.878883
1	17	6916998.15	427997.92	140.268583	-27.869867
1	18	6918000.75	428001.78	140.268683	-27.860817
1	19	6918996.04	428005.69	140.268783	-27.851833
1	20	6920009.49	427971.78	140.2685	-27.842683
2	1	6915006.41	422998	140.217667	-27.887567
2	2	6914985.18	424016.92	140.228017	-27.887817
2	3	6914998.73	424996.24	140.237967	-27.88775
2	4	6914997.47	425993.67	140.2481	-27.887817
2	5	6915001.81	426995.98	140.258283	-27.887833
2	6	6914991.64	429002.48	140.278667	-27.888033
2	7	6915006.63	429993.21	140.288733	-27.88795
2	8	6915026.58	430993.85	140.2989	-27.887822
2	9	6915001.48	431996.32	140.309083	-27.8881
2	10	6914984.91	432993.91	140.319217	-27.8883
2	11	6914990.07	433989.9	140.329336	-27.888303
2	12	6914994.02	435002.92	140.339628	-27.888317
2	13	6915001.23	435997.52	140.349733	-27.8883
2	14	6914997.26	436990.11	140.359817	-27.888383
2	15	6914992.91	437988.9	140.369964	-27.888469
2	16	6915002.01	438990.08	140.380136	-27.888433
2	17	6914999.95	439991.9	140.390314	-27.888497
2	18	6915000.92	440998.04	140.400536	-27.888533
2	19	6915001.99	441993.54	140.41065	-27.888567
2	20	6914999.47	442997.53	140.42085	-27.888633
2	21	6915000.16	443997.16	140.431006	-27.888669
2	22	6914971	446056.9	140.451931	-27.889017
2	23	6914997.37	447005.23	140.461567	-27.888817

APPENDIX B: ADDITIONAL INFORMATION – PART II

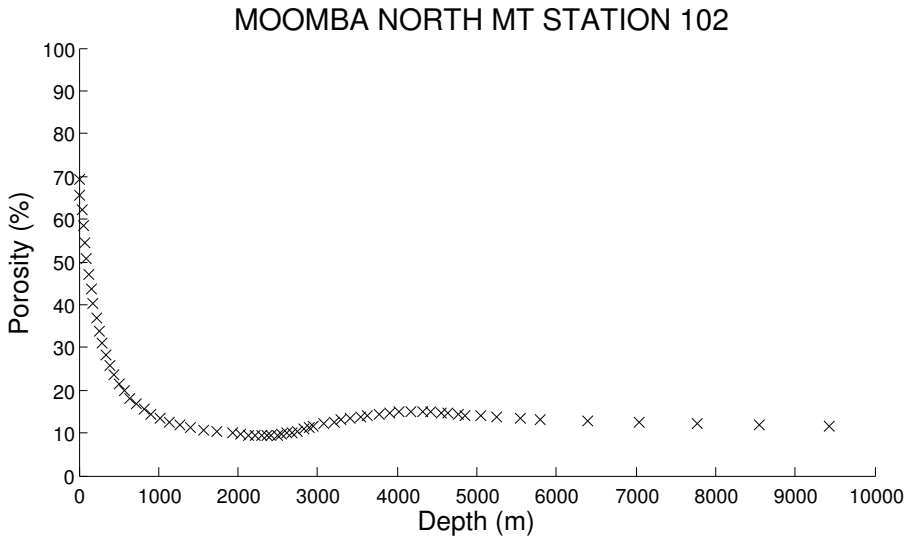

Figure 18: Porosity at the Moomba North MT survey station 102. Station 102 is the closest site in the survey to the Moomba 086 borehole. The porosity was calculated using Archie's law. The depth shown ranges from 0-10000 m to show that Archie's law starts to fail at $\approx$ 3000-4000 m.

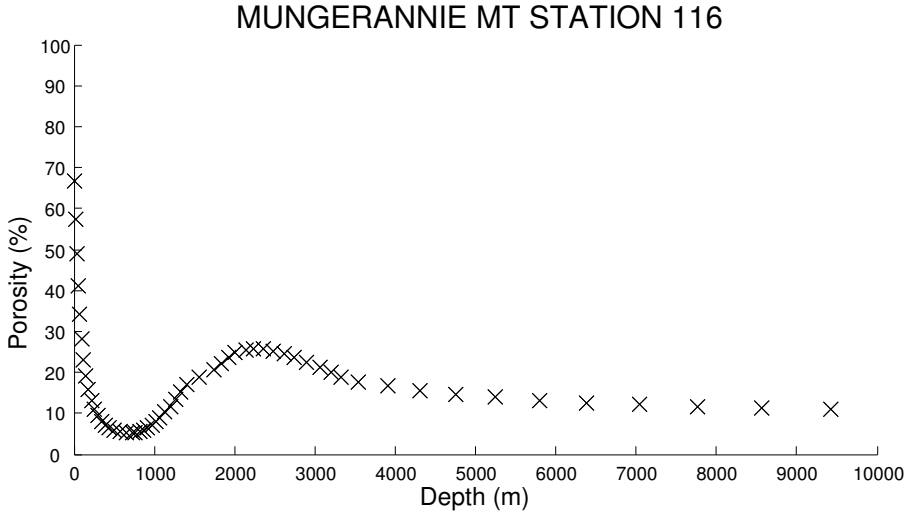

Figure 19: Porosity at the Mungerannie MT survey station 116. Station 116 is the closest site in the survey to the Mulkurra West 001 borehole. The porosity was calculated using Archie's law. The depth shown ranges from 0-10000 m to show Archie's law failing between 2000-3000 m due to the presence of basement rocks.